Permanent Polymer Coating for in vivo MRI Visualization of Tissue Reinforcement Prostheses

Olivier Guillaume, Sébastien Blanquer, Vincent Letouzey, Arnaud Cornille, Stéphanie Huberlant, Laurent Lemaire, Florence Franconi, Renaud de Tayrac, Jean Coudane, Xavier Garric

Permanent Polymer Coating for in vivo MRI Visualization of Tissue Reinforcement Prostheses[a]

Olivier Guillaume, Sébastien Blanquer, Vincent Letouzey, Arnaud Cornille, Stephanie Huberlant, Laurent Lemaire, Florence Franconi, Renaud de Tayrac, Jean Coudane, Xavier Garric*

The clinical advantage of MRI visualization of prostheses in soft tissue prolapses is very appealing as over 1 000 000 MRI-transparent synthetic meshes are implanted annually, and postoperative complications such as mesh shrinkage and migration are frequent. Here, the synthesis of a new material composed of a DTPA-Gd complex grafted onto a backbone of PMA via a covalent bond is described (DTPA-Gd-PMA). This new polymer is sprayed onto meshes and gives an MR signal for a long period without any significant release of Gd. In vitro cytocompatibility tests on fibroblasts show limited cytotoxicity. Microscopic investigations indicate that vital cells rapidly colonize the material. Finally, coated meshes implanted in rats are easily recognizable using an MR imaging system.

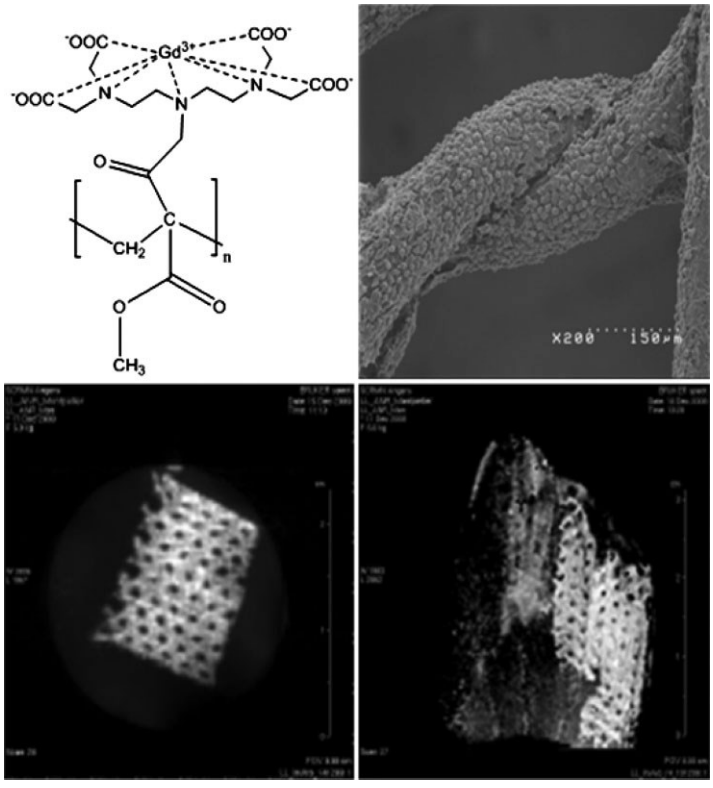

Dr. O. Guillaume, Dr. S. Blanquer, Dr. V. Letouzey, A. Cornille, S. Huberlant, Prof. J. Coudane, Dr. X. Garric
Max Mousseron Institute of Biomolecules (IBMM), UMR CNRS 5247, University of Montpellier 1, University of Montpellier 2, Faculty of Pharmacy, 15 Av. C. Flahault, Montpellier 34093, France
E-mail: xavier.garric@univ-montp1.fr
Dr. V. Letouzey, A. Cornille, S. Huberlant, Prof. R. de Tayrac
Obstetrics and Gynaecology Department, Caremeau University Hospital, Nˆımes 30100, France

Dr. L. Lemaire, Dr. F. Franconi
LUNAM University, UMR-S646, Angers 49933, France
Dr. L. Lemaire
Micro- et Nanomédecines Biomimétiques - MINT, Angers 49933, France

[a] Supporting Information for this article is available from the Wiley Online Library or from the author.

1. Introduction

Magnetic resonance imaging (MRI) is today the most powerful non-invasive technique that can be used to provide high spatial and temporal resolutions without ionizing radiation. This imaging tool is widely used for the clinical diagnosis and/or staging of human diseases.[1,2] Unfortunately, it isunableto provide a postoperative image of implanted prostheses.[3–6]

A new MRI-visible prosthesis would therefore be most appealing for the clinical follow-up of patients undergoing soft tissue reinforcement surgery (i.e., for vaginal prolapse, hernia wall repair, or urinary incontinence) and would be of great benefit to surgeons and radiologists. Thus, clinicians would be informed about the exact localization of the prosthesis, its tissue integration and any changes in its size or shape. Most of the surgical meshes implanted are made of poly(propylene) (PP), polyester (PET), polytetrafluoroethylene or its expanded form (PTFE and ePTFE, respectively).[7–9]

To the best of our knowledge, few researchers have succeeded in creating a long-term MRI-visible medical device. Some studies have focused on materials that can enhance MRI contrast by using ferrous superparamagnetic particles.[10–13] Unfortunately, these ferrous-based products are negative contrast agents (T_2/T_2^{ω} agents) that induce less enhancement of the signal that positive contrast agents (T_1 agents). It therefore follows that the MRI signal enhancement they induce is not sufficient to localize the material implanted in soft organs composed of muscle fibers and connective tissue.[14] Positive contrast agents contain paramagnetic elements (e.g., gadolinium) and are generally injected prior to MRI scanning in order to increase the signal. Higher image resolution is obtained by modulating the relaxation time of the water protons in the tissue.[15]

Gadolinium-based contrast agents encapsulated in polymer micro or nanoparticles have already been described.[16–18] Their main drawback is that they provide only short-term visualization due to the gadolinium released into the surrounding media. Unal has presented several diethylenetriaminepentaacetic acid (DTPA)-Gd entrapment strategies that are intended to create an MRI-visible hydrogel on endovascular devices. However, only short-term MRI visibility was reported.[19] Other authors have chemically grafted contrast agents onto several polymers, but using labile and hydrolyzable ester or amide bonds. These strategies may not allow for long-term clinical application because the contrast agent may be cleaved and released from the polymer.[20–23]

The study described here aimed to synthesize a new MRI visible polymer composed of a DTPA-Gd complex grafted onto a backbone of poly(methyl acrylate) (PMA) via a covalent and non-labile bond (DTPA-Gd-PMA). The characterization of all the compounds generated, and all by-products and final polymer, is reported herein. In addition, thepotential of thisnon degradable MRI-visiblepolymerfor biomedical applications was investigated by (i) assessing the device's MR visibility and the stability of the $Gd^{3þ}$ polymer complex, (ii) evaluating the effect of irradiating or gas sterilization processes on MR signal and complex stability, (iii) determining the cytocompatibility of this new polymer and its possible toxicity. Finally, after implantation in rats, the MR signal of DTPA-Gd-PMA-coated meshes was evaluated in vivo on a 7 T MRI Scanner.

2. Experimental Section

2.1. Materials

PMA ($\overline{M}_w$ ¼ 40 000 g · mol^{-1}, 40% w/v in toluene) was obtained from Aldrich (St Quentin Fallavier, France), benzyl alcohol (purity ¼ 99%) and palladium on activated carbon (10% Pd) were purchased from Acros (Gell, Belgium). $MgSO_4$ and DTPA dianhydride (DTPA-diA) were supplied by Carlo Erba (Milano, Italy) and were used as received.

Lithium diisopropylamide (LDA) [2 M in tetrahydrofuran (THF)/heptane]; gadolinium (III) chloride hexahydrate (99%), thionyl chloride ($SOCl_2$), dried THF; dichloromethane, diethyl ether, methanol, and dry dimethyl sulfoxide were purchased from Sigma-Aldrich (St-Quentin Fallavier, France). All chemicals and solvents were used without further purification except THF which was treated over benzophenone sodium then distilled.

Polymer molar masses were determined by size exclusion chromatography (SEC) on a Waters Inc. system fitted with a PLgel 5 mm mixed-C (60 cm) column (Polymer Laboratories, Les Ulis, France) anda Waters 410 refractometric detector. THFmobilephase was eluted at room temperature at 1 mL · min^{-1}. Typically, polymer samples were dissolved in THF (10 mg · mL^{-1}), and 20 mL were injected. The SEC system was calibrated using polystyrene standards. A Waters PDA 2996 photodiode array detector (PDA) was added online for the specific detection of aromatic groups.

Attenuated total reflectance Fourier-transform infrared (ATR-FTIR) spectra were obtained for polymer films cast on NaCl and recorded on a Perkin-Elmer Spectrum 100 FTIR spectrometer using ATR.

^{1}H NMR spectra were recorded in deuterated dimethyl sulfoxide (DMSO-d_6) on an AMX300 Bruker spectrometer operating at 300 MHz. Chemical shifts were expressed relative to tetramethylsilane (TMS).

Relaxation times for polymers dissolved in DMSO-d_6 were measured on a BrukerAMX400 spectrometer operating at 400 MHz. This analysis was carried out at 80 8C to facilitate polymer molecular mobility.

$Gd^{3þ}$ was quantified using an Element XR sector field inductively coupled plasma mass spectrometer (ICP-MS) at Geosciences in Montpellier (Montpellier II University). Internal standardization used an ultra-pure solution spiked with Indium.

2.2. Synthesis and Characterization of the MRI-Visible Polymer DTPA-Gd-PMA

2.2.1. Synthesis of Benzylated DTPA (Bn2-DTPA)

Commercial DTPA-diA (14 mmol, 5 g) was dispersed in DMSO (20 mL) and benzyl alcohol (35 mmol, 3.6 mL) was added for complete dissolution of the mixture within a few hours. The reaction was monitored by infrared analysis until total disappearance of the anhydride band at 1820 cm^{-1}. After 5 h the DMSO was evaporated off. The residue was precipitated and washed with diethyl ether.

2.2.2. Chlorination of DTPA-Bn2 (Bn2-DTPA-Cl)

The Bn_2-DTPA powder (5.3 mmol, 3 g) was dissolved in thionyl chloride (5 mL). The reaction was conducted at room temperature for 2 h under a flow of argon, and was followed by monitoring the intensity of the band at 1795 cm^{-1}.

2.2.3. Reaction of Bn2-DTPA-Cl with PMA-(Bn2-DTPA-PMA)

A solution of PMA (35 mmol, 3 g) in anhydrous THF (200 mL) was cooled ina dried reactor at −30 °C usinga mixture of liquidnitrogen and ethanol. The solution was carefully maintained under a flow of dry argon while stirring. A 2 M LDA solution (104.6 mmol, 52 mL) was poured through a septum into the solution for 30 min while stirring. Bn_2-DTPA-Cl (6.5 mmol, 4.1 g) was dissolved in dry THF and rapidly injected into the solution of PMA^- through a cannula, and the mixture was gradually returned to 0 °C in 1 h. It was then neutralizedwithan aqueous solutionof 0.1 N HClto a pHof 2–3, and extracted twice with dichloromethane (200 mL). The combined organic phases were washed with distilled water (200 mL) and dried on anhydrous $MgSO_4$. After filtration, the dichloromethane was partially evaporated off under vacuum and Bn_2-DTPA-PMA was precipitated in diethyl ether. Finally, the precipitate was dissolved and purified by dialysis in CH_2Cl_2/MeOH using Spectra/Por membrane tubing (cut-off: 3500 Da). The copolymer was finally recovered by precipitation in diethyl ether.

2.2.4. Synthesis of DTPA-PMA

A solution of Bn_2-DTPA-PMA (1.5 g) in THF was subjected for 3 d to a H_2 pressure of 5 bar in the presence of 10% Pd/C at room temperature while stirring vigorously. The catalyst was removed by filtration over celite and the copolymer was recovered by precipitation in diethyl ether.

2.2.5. Synthesis of DTPA-Gd-PMA

Asolutionof $GdCl_3$ (800 mg) in DMSO(2 mL) wasaddedto asolution of DTPA-PMA (1 g) in DMSO (5 mL). The mixture was then heated to 80 °C and stirred for 48 h. The DMSO was then evaporated off under vacuum, CH_2Cl_2 (50 mL) was added and the solution was washed twice with H_2O (25 mL). The organic phase was removed and dialyzed against a mixture of MeOH/CH_2Cl_2 50:50 v/v until no gadolinium was detected by ICP-MS in the external dialysis phase. The DTPA-Gd-PMA copolymer was recovered after precipitation in diethyl ether.

2.3. In vitro MR Visualization, Stability Study and Effect of Sterilization Process

3 × 3 cm^2 monofilament PP meshes were coated using an Infinity Airbrush system supplied by Harder & Steenbeck (Oststeinbek, Germany). Asolutionof DTPA-Gd-PMA/poly(methylmethacrylate) (PMMA, 1:9 w/w) in acetone (1% w/v) was sprayed onto the PP meshes under 3 bars of argon pressure from a distance of 5 cm. The meshes were dried in a vacuum overnight and weighed to measure the amount of coated polymer.

DTPA-Gd-PMA coated meshes were sterilized by 25 kGy of gamma radiation in an ambient atmosphere (g ray) or a nitrogen atmosphere (g ray N) (5.87 kGy · h^{-1} from a ^{60}Co source), or by ethylene oxide (EO) at 51 °C (Sterlab, Vallauris, France).

MR signalenhancement efficiencyof the MR-visible meshes was determined at T0 and after 13 and 27 weeks of immersion in phosphate-buffered saline (PBS) at 37 °C with stirring at 130 rpm (Heidolph Unimax 1010, Schwabach, Germany). MR images were acquired on a Bruker Avance DRX system (BrukerBiospin SA, Wissembourg, France) operatinga Paravision(version 4.0) software platform. The system is equipped with a 150 mm vertical super-wide-bore magnet operating at 7 T, a 84 mm inner diameter shielded gradient set capable of 144 mT · m^{-1} maximum gradient strength and a 30 mm diameter birdcage resonator. Meshes (1 cm^2) were embedded in degassed 1 wt% agar gel prior to imaging. Gadolinium-free samples corresponded to a native PP mesh. Signal enhancement was tested by introducing T_1 weighting into the MR images using an inversion pulse in a rapid 3D acquisition with a relaxation enhancement (RARE) sequence [TR ¼ 2000 ms; mean echo time (TEm) ¼ 31.7 ms; RARE factor ¼ 8; FOV ¼ 3 × 3 × 1.5 cm^3; matrix 128 × 128 × 64].[24] The inversion delay was set at 1300 ms, sufficient to allow the signal from the embedding gel to disappear.

Gadolinium release from DTPA-Gd-PMA coated mesh was compared with that of a positive control made up of a mesh coated successively with a solution of Magnevist (Gadopentetatedimeglumine, Bayer, Germany) and a solution of PMA. Released gadoliniumwasquantifiedby ICP-MSatdifferenttimepoints(1, 13, and 27 weeks) after mesh immersion in 10 mL of PBS at 37 °C and stirred at 130 rpm. At each scheduled time point, 1 mL of the PBS solution was replaced by fresh buffer and Gd was measured by ICP-MS. All time points correspond to measurements in triplicate. After 6 months, the meshes were degraded by exposure for 2 d 65% HNO_3 at 150 °C. They were then dissolved in 10 mL of dilute HNO_3 and Gd was quantified by ICP-MS.

2.4. In vitro Cytocompatibility of DTPA-Gd-PMA Films

2.4.1. Culture of Murine Fibroblasts

Cytocompatibility tests were conducted on the L-929 fibroblast cell line. Murine L-929 cells were cultured in Eagle's minimum essential medium (MEM) supplemented with 10% foetal horse serum (FHS), 1% penicillin solution (10 000 U · mL^{-1}), 10 mg · mL^{-1} streptomycin (PenStrep), and 1% glutamine GlutaMAX-1. All tissue culture reagents were purchased from Gibco Invitrogen (Cergy Pontoise, France). Cells were grown in 75 or 175 cm^2 cell culture flasks to approximately 80% confluency in a 5% CO_2 incubator at 37 °C.

2.4.2. Preparation of Polymer Films

MR-visible polymer (10% DTPA-Gd-PMA diluted in PMMA) and the gadolinium-free polymer control (10% PMA diluted in PMMA) were dissolved in acetone and sprayed directly onto the surface of 24-well culture plates (Falcon, Becton Dickinson, Le Pont De Claix, France). The plates were then dried under vacuum overnight and sterilized by 25 kGy gamma radiation.

2.4.3. 3-(4,5-Dimethylthiazol-2yl)-2,5-diphenoltetrazolium Bromide (MTT) Test

An MTT test, supplied by Euromedex (Souffelweyersheim, France), was performed to determine cells vitality by their mitochondrial dehydrogenase activity. 100 000 L-929 fibroblasts were seeded and allowed to adhere to the well surface for 15, 30, and 60 min. The wells were then washed once by dynamic dipping into Dulbecco's phosphate-buffered saline (D-PBS) before the MTT test was conducted. Cell proliferation was determined by seeding 24-well culture plates with 5 000 L-929 fibroblasts and allowing to stand for 30 min before adding culture medium. MTT tests were performed on days 1, 4, and 6 post-seeding. All MTT tests were performed in accordance with the literature.[25,26] Briefly, 250 mL of an MTT solution(1 mg · mL^{-1} in D-PBS) wereadded to thewellsandafter 3 h of incubation the reagent was removed, the wells were washed with D-PBS, and isopropyl alcohol was added to dissolve the formazan. Formazan was measured at 570 nm using a spectrophotometer multiplate reader (Victor*X*3 multilabel plate reader, Perkin-Elmer). L-929 fibroblast adhesion and proliferation were tested in triplicate.

2.4.4. Titration of Lactate Dehydrogenase (LDH)

PromoKine's LDH Cytotoxicity Assay Kit II, supplied by PromoCell GmbH (Heidelberg, Germany), was adapted according to their recommended procedure. On d 6 of L-929 fibroblast growth on the polymer-coated surfaces, 10 mL of the 1 mL supernatant were transferred directly in triplicate into an optically clear 96-well plate (Positive control consisted of 10% Cell Lysis Solution in wells containing L-929 cells). 100 mL of reconstituted test solution were addedto the 10 mLofthesupernatant, mixedandincubatedatroom temperature for 30 min. The absorbance was measured at 450 nm using a spectrophotometer multiplate reader.

2.4.5. Quantification of Interleukin-6 (IL-6)

135 000 L-929 cells were seeded onto the surface of each polymer-coated well with 1 mL of culture medium. Controls corresponded to tissue-culture treated polystyrene supplemented or not with *Escherichia coli* lipopolysaccharide at 10 mg · mL^{-1} (LPS 0127:B8, Sigma), a product that induces an inflammatory response. After 48 h, cell culture supernatants were collected in tubes, centrifuged at 6000 rpm for 5 min and stored at —80 8C pending analysis. At the same time, the L-929 cells were treated with trypsin (trypsin-EDTA used at 0.05%) and counted in each well in a Thoma-Zeiss counting chamber.

IL-6 was detected and measured using a Mouse IL-6 ELISA Set (BD OptEIA) purchased from BD Sciences (San Diego, CA, USA) following the recommended assay procedure. IL-6 supernatant was performed in triplicate for each well and results are expressed in pg · mL^{-1} of IL-6 secreted for 100 000 L-929 cells.

Results are presented as mean SD and differences between groups were studied by one-way analysis of variance (ANOVA, StatGraphic). We considered $p < 0.05$ to be statistically significant.

2.5. In vitro Colonization of MR-Visible Meshes

15 mm diameter disks of native PP meshes, MR-visible polymer (DTPA-Gd-PMA/PMMA) and Gd-free polymer (PMA/PMMA) coated meshes (obtained by the airbrush technique using the protocol already described) were stirred for 2 h on a roller mixer at 33 rpm (supplied by Labo-moderne, Paris, France) at 37 8C in tubes containing culture medium and 500 000 L-929 cells · mL^{-1}. The meshes were then transferred to 24-well culture plates and washed in D-PBS to eliminate non-adhesive cells. An MTT test was performed as previously described in triplicate to determine initial cell adhesion. On day 8, cell's viability on meshes was evaluated using PromoKine's Live/Dead Cell Staining Kit I (PromoCell GmbH, Heidelberg, Germany) by adding 250 mL of the live/dead stain followed by incubation of the mixture at 37 8C for 15 min. Cell staining was observed under a confocal microscope (Leica Macroconfocal LSI microscope, Nanterre, France).

The meshes were further examined by scanning electron microscopy (SEM, Hitachi 400, Sophia Antipolis, France). To do this, the meshes were removed from the culture medium on day 8, then washed. The cells were fixed with 3.3% glutaraldehyde in Milloning's phosphate buffer and dehydrated by successive 30–70% ethanol baths followed by critical point drying with CO_2. The meshes were then sputter coated with an approximate 10 nm thick gold film and examined by SEM using a lens detector with a 10 kV acceleration voltage at calibrated magnifications.

2.6. In vivo Mesh Visualization on an Experimental MRI Apparatus

MR-visible meshes coated with DTPA-Gd-PMA/PMMA containing 20 or 30 mg Gd were prepared by airbrushing PP meshes then sterilized by 25 kGy of gamma radiation. A negative control consisted of PMA/PMMA-coated mesh.

Wistar rats were housed in the Nˆımes University experimental research center. The experiment described herein was accepted by University's Animal Research Ethics Committee (CEEA-LR-1010).

Rats were anesthetized with isoflurane and their dorsal fur was shaved off. The exposed skin was then cleaned with 10% povidone/iodinesolution. 2-cmincisionsweremadeoneachsideof the backbone. Two pieces of MR-visible mesh were implanted subcutaneously (1.5 × 2 cm^2) and on the lumbar muscle (1 × 2 cm^2) on the left side and fixed with sutures. Negative controls were similarly implanted but on the right side. The skin incision was then closed by sutures. The animals were checked daily during the observation period to detect any local or systemic complications. After 1 month, MR images of the implanted rats were obtained under isoflurane anesthesia on a 7 T Bruker Avance DRX system.

3D T_1-weighted spoiled gradient echo images were acquired with 100 ms repetition time, 3 ms echo time, a 758 flip angle, a 30 × 30 × 10 mm^3 field-of-view of and a 64 × 64 × 32 matrix. Two experiments were conducted and imaging time was 11 min. Maximum intensity projections (MIPs) were then processed from the 3D dataset.

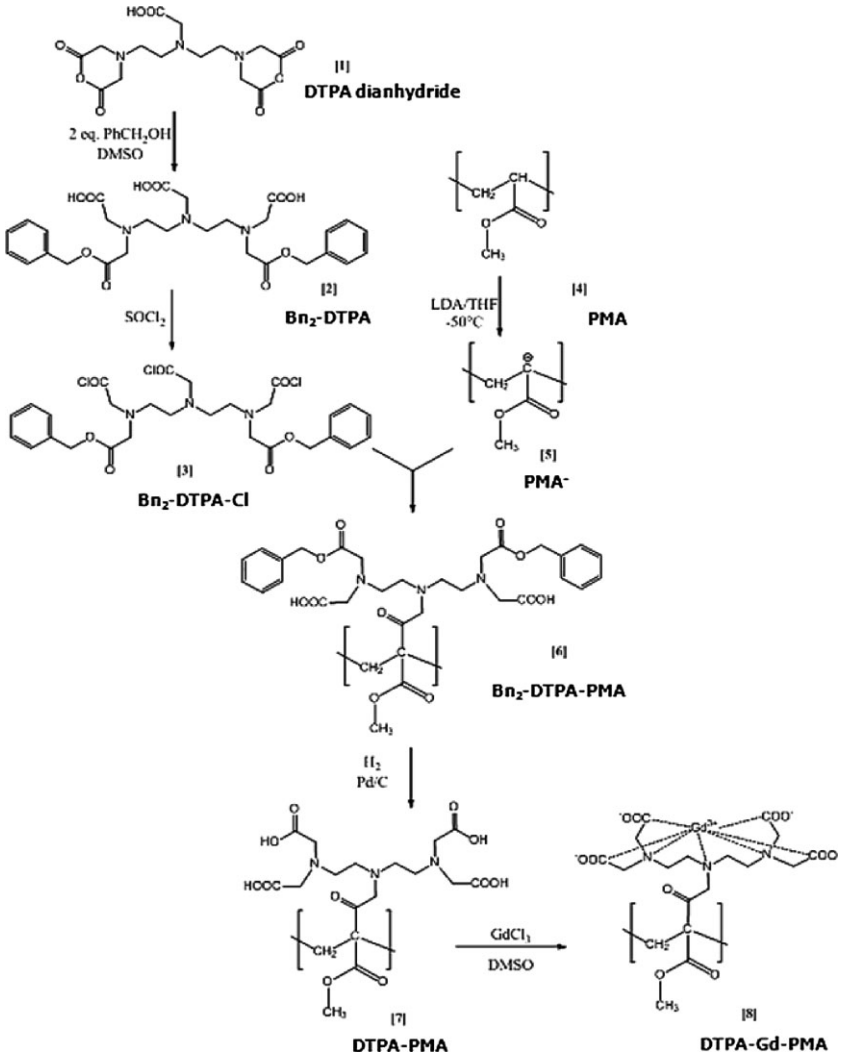

Scheme 1. Synthesis of DTPA–Gd–PMA by the anionic modification method. (Product 6 corresponds to a schematic representation. The position of the carboxylic acid functions obtained after the reaction was not determined).

3. Results and Discussion

3.1. Synthesis and Characterization of DTPA-Gd-PMA

Gd^{3+}-containing polymer complexes were prepared as illustrated in the Scheme 1. The DTPA ligand was grafted to the PMA chain by anionic modification according to a previously described method.[27]

This strategy has been developed in particular for PCL in order to provide functionalized structures.[28–30]

Inorder to graftthe DTPAchelate onto thepolycarbanion, it is necessary to activate DTPA under an acid chloride form. As DTPAisinsoluble inorganic solvents, itmustbe modified before this reaction can take place. DTPA-diA (1) was therefore esterified with benzyl alcohol in a quantitative manner to yield Bn_2-DTPA (2), which is soluble in organic solvents (i.e., THF) as well as in thionyl chloride which was used as solvent in the chlorination step (3).

Bn_2-DTPA (2) purity was checked by high-performance liquid chromatography (HPLC) and its structure was determinedby ^{1}HNMR(Figure S1) andelectron spray ionization mass spectrometry (ESI-MS) ([M þ H]$^+$ ¼ 574.3 Da).

NMR peak assignments for Bn_2-DTPA were as follows: δ ¼ 2.9 (m, 8H, CH_2-N); 3.4 (s, 6H, CH_2-COOH); 3.6 (s, 4H, CH_2-COO-Bn); 5.1 (s, 4H, CH_2-Ph); 7.3 (m, 10H, aromatic protons).

Bn_2-DTPA was then activated by reaction with thionyl chloride at room temperature. The reaction was monitored by FTIR using the acid chloride band at 1795 cm^{-1} in the activated Bn_2-DTPA-Cl (3) (Figure S2).

The presumed structure of Bn_2-DTPA-Cl consists of three acyl chloride groups. Given that Bn_2-DTPA-Cl is very unstable, it was used immediately for the next step after evaporation of thionyl chloride, without further purification.

Bn_2-DTPA-Cl was added to the polycarbanion (5) to give Bn_2-DTPA-PMA (6), which was recovered by precipitation in diethyl ether and purified by dialysis in CH_2Cl_2/MeOH 50:50 v/vusingtubes with a cut-off of 3500 Da.

Bn_2-DTPA-PMA was characterized and its purity determined by ^{1}H NMR, 2D-DOSY NMR and SEC using dual refractometric/PDA detection. SEC/PDA showed that PMA does not absorb at $>$290 nm whereas Bn_2-DTPA-PMA (retention time 15.5 min) absorbs at $>$290 nm, demonstrating conclusively the presence of grafted benzyl groups on the polymer skeleton (Figure 1A). No peaks appeared at elution time $>$15.5 min, showing that no small molecules were present in the sample. Bn_2-DTPA grafting and Bn_2-DTPA-PMA purity were confirmed by diffusion-ordered 2D NMR spectroscopy (DOSY) with a single diffusion coefficient on the DOSY spectrum.

Degree of substitution of Bn_2-DTPA on PMA was measured by ^{1}H NMR along with the ratio integration of aromatic groups at δ ¼ 7.3 divided by the integration of methyl group on the PMA skeleton at δ ¼ 3.7 (Figure 1B). The degree of substitution was 3–4%. This low value is probably a consequence of the steric hindrance and instability of Bn_2-DTPA-Cl.

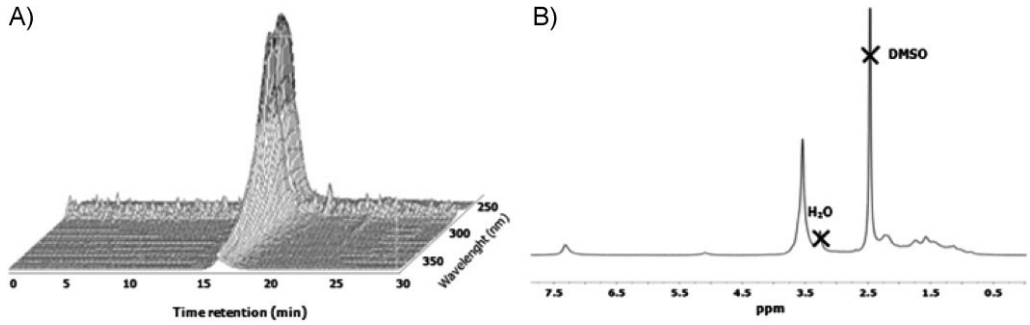

Figure 1. 3D SEC chromatograms of Bn_2–DTPA–PMA solutions in THF (A). ^{1}H NMR spectrum of Bn_2–DTPA–PMA in DMSO-d_6 (B).

To allow for optimal gadolinium complexation, benzyl groups were cleaved by catalytic hydrogenolysis in THF, in the presence of Pd (10%) on charcoal (7). The efficiency of this deprotection was checked by ^{1}H NMR which showed that no benzyl groups were present in final DTPA-PMA. ^{1}H NMR peak assignments for Bn_2-DTPA-PMA were as follows: δ ¼ 1.7–2.1 (t, 3H, CH_2; CH_2-CH); 3.7 (s, 3H, CH_3); 5.1 (s, 4H, CH_2-Ph); 7.3 (m, 10H, aromatic protons).

Finally, gadolinium complexation was carried out by the reaction of excess $GdCl_3$ with DTPA-PMA in DMSO at room temperature (8). Free gadolinium was eliminated by successive washings in MeOH/CH_2Cl_2 50:50 until no gadolinium was detected by ICP-MS. The degree of complexation (proportion of complexed Gd/number of grafted DTPA) was 50%. This low value may be explained by the difficulty to find an ideal solvent for both $GdCl_3$ and PMA-DTPA. The polymer is probably folded up and the access to grafted DTPA for $Gd^{3þ}$ is tricky. As gadolinium interfered with the NMR spectrum, the effect of grafted gadolinium was measured by determining the T_1 relaxation time for the only distinguishable protons, i.e. those on the methyl groups of the PMA backbone. Methyl group proton relaxation time was substantially shorter when DTPA/PMA was complexed with gadolinium (0.082 s), than for the gadolinium-free polymer (1.56 s).

3.2. In vitro MR Visualization, Stability Study, and Effect of Sterilization Process

DTPA-Gd-PMA was coated onto commercial PP meshes (3 × 3 cm^2) usinganairbrushsystem. Thispolymer wasadded to a 1% (w/v) solution of PMMA in acetone as this was found to result in mesh coating that neither broke nor peeled. Figure 2 and Video 1 (available in the Supporting Information) illustrate the MRI visualization provided by DTPA-Gd-PMA (substitution ratio of 2%) coated onto a commercial mesh used in the repair of genital prolapse. DTPA-Gd-PMA-coated meshesweresclearlyvisible intheagargelfor 27 weeks, while uncoated meshes did not show any contrast enhancement.

The effect of sterilization on MR signal enhancement was also investigated. Three sterilization processes, namely 25 kGy gamma radiation in an ambient atmosphere (Gamma), under nitrogen (Gamma N), or by exposure to ethylene oxide (EO) at 51 8C, were chosen as these are routinely used in the medical device industry. The mesh-induced enhancement of the MR T1 signal was assessed over time after sterilization and compared with native DTPA-Gd-PMA-coated meshes. The results showed that the MR signal enhancement was conserved for at least 27 weeks, and this for all three sterilization processes (Figure 2).

Figure 3 illustrates the necessity to graft the contrast agent (DTPA-Gd) onto the PMA polymer backbone to avoid gadolinium release. Asa further illustration, when PP meshes were coated with DTPA-Gd (Magnevist) dispersed in PMA/PMMA(1:9 w/w), 98% of the gadoliniumwas released within 1 week. The stability study shows that decomplexation phenomenon of Gd from the DTPA-Gd-PMA-coated mesh is marginal. Indeed, even after 6 months ofimmersion in PBS at 37 8C, only 5 mgofgadolinium were released fromthe meshes corresponding to less than 3% of the initial amount of gadolinium. Moreover, none of the sterilization processes to which the coated meshes were subjected increased the release of gadolinium. Similarly, Frenzel et al. indicated that around 2% of $Gd^{3þ}$ were decomplexed from Magnevist after 2 weeks of incubation in vitro.[31]

Whendealingwithgadolinium-based contrastagent, the question usually arises of associated nephrogenic systemic fibrosis disorder (NFS) in patients with renal failure. However, it is noteworthy that this phenomenon is usually observed after a conventional MR scan where patients receive 1 g gadolinium as a bolus.[32,33] In the present case, an evident T_1 enhancement was observed with a mesh loaded with about 1 mg · cm^{-2} which corresponds, for a 100 cm^2 implanted mesh, to only 0.01% of the dose given during a conventional scan.

3.3. In vitro Cytocompatibility of DTPA-Gd-PMA Films

The cytocompatibility of the MR-visible polymer (DTPA-Gd-PMA/PMMA) was evaluated by in vitro adhesion and proliferation tests (Figure 4). L-929 cells were chosen for the tests as recommended by ISO specifications and especially

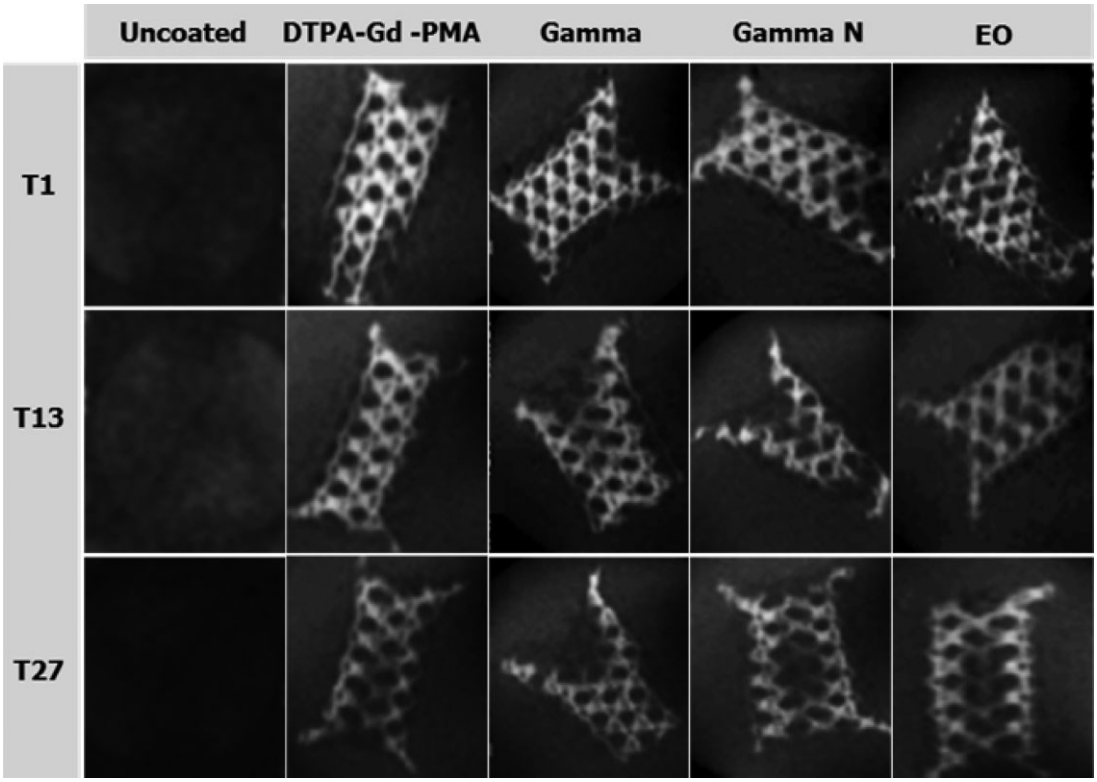

Figure 2. MR images of DTPA–Gd–PMA–coated meshes before and after sterilization by gamma radiation in ambient atmosphere (Gamma), under nitrogen (Gamma N), or by exposure to EO at 51 8C (EO). MR signal persistence was assessed after 1, 13, and 27 weeks of stability testing in PBS at 37 8C. Uncoated mesh served as negative control. Signal enhancement was tested by introducing T1 weighting into the MR images using an inversion pulse in a rapid 3D acquisition with a relaxation enhancement (RARE) sequence [TR ¼ 2 000 ms; mean echo time (TEm) ¼ 31.7 ms; RARE factor ¼ 8; FOV ¼ 3× 3 × 1.5 cm^3; matrix 128 × 128 × 64].

for the evaluation of medical device cytotoxicity.[34] The overall results showed that L-929 adhesion after 15 and 60 min was significantly greater for the Gd-free and MR-visible polymers than for the tissue-culture polystyrene (TCPS) control (Figure 4A).[30] Cell adhesion for both Gd-free (PMA/PMMA) and MR-visible(DTPA-Gd-PMA/PMMA) polymers wasnot time-dependent as maximal MTT values were reached after only 15 min. These two polymer surfaces showed similar cell proliferation profiles, but both were significantly lower than the TCPS control ($p < 0.05$). Differences in terms of L-929 proliferation capabilities were mainly observed on day 6 with MTT results of 1.81, 0.86, and 0.50 for TCPS, Gd-free, and MR-visible polymers, respectively (Figure 4B).

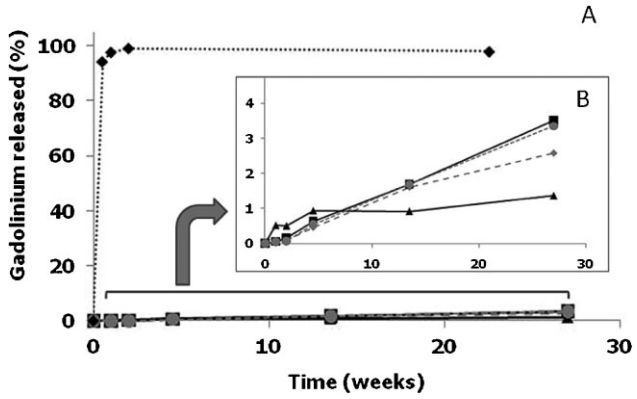

Figure 3. (A) Release of gadolinium from a mesh coated with a mixture of Magnevist/PMA (◆); from meshes coated with DTPA–Gd–PMA before (◇) and after sterilization by gamma radiation in an ambient atmosphere (Gamma —■—), under nitrogen (Gamma N —▲—) or exposure to EO at 51 8C (EO ···●···). (B) Enlargement of Figure 3A representing the release of gadolinium from coated meshes before and after sterilization.

Interleukin-6 (IL-6) and LDH were then measured to determine whether these two polymers may be considered as cytotoxic. The results showed that IL-6 was over-expressed in the LPS positive control. By contrast, the MR-visible polymer (DTPA-Gd-PMA/PMMA) did not induce an inflammatory response in L-929 cells as no significant differences were observed compared to the TCPS control (Figure 4C).

Lactate dehydrogenase (LDH) released from damaged cells is commonly titrated to evaluate the cytotoxicity of a material or soluble drug. After 6 d of incubation, the MR-visible polymer did not induce a significantly higher LDH

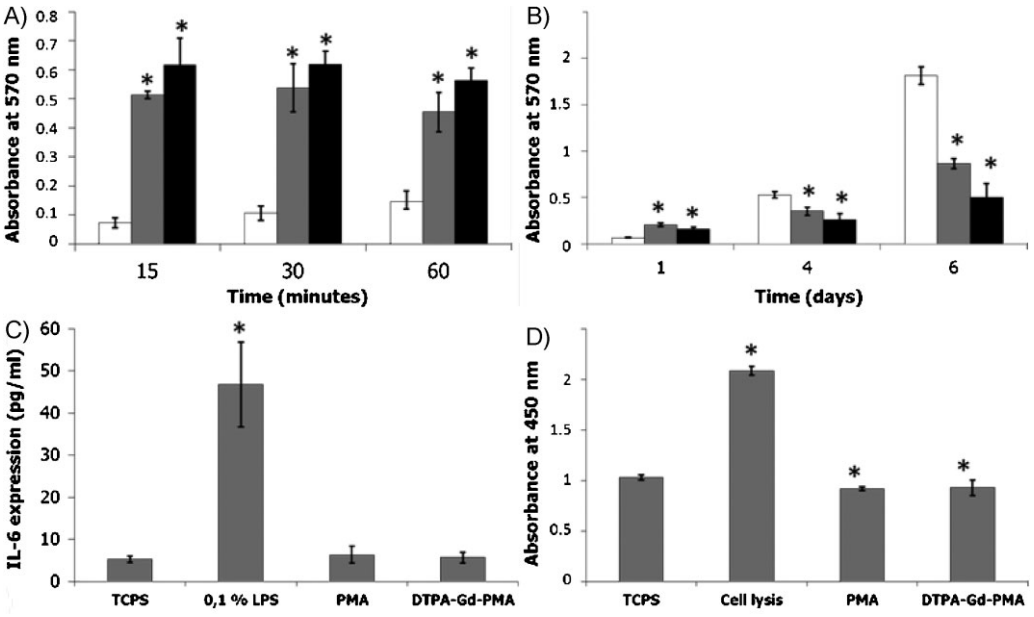

Figure 4. Adhesion (A) and proliferation (B) of L-929 cells on TCPS (□), PMA/PMMA (▨) and DTPA-Gd-PMA/PMMA (■) plus inflammatory response evaluated by IL-6 release (C) and LDH titration on day 6 (D). Results correspond to absorbance values of violet formazan at 570 nm (A and B for MTT test) and absorbance values of red formazan at 450 nm (D for LDH test). Statistical analysis performed with TCPS as reference ($^{\omega}$ represents a p value <0.05). All data points and standard deviations are the result of triplicate experiments.

release rate in the culture medium compared to PMA/PMMA (Figure 4D). In addition, neither of the two polymers affected cell alteration as their respective response values were similar to those of the negative control (TCPS; abs. ¼ 1.0) and lower than the positive control (TCPS þ cell lysis; abs. ¼ 2.0).

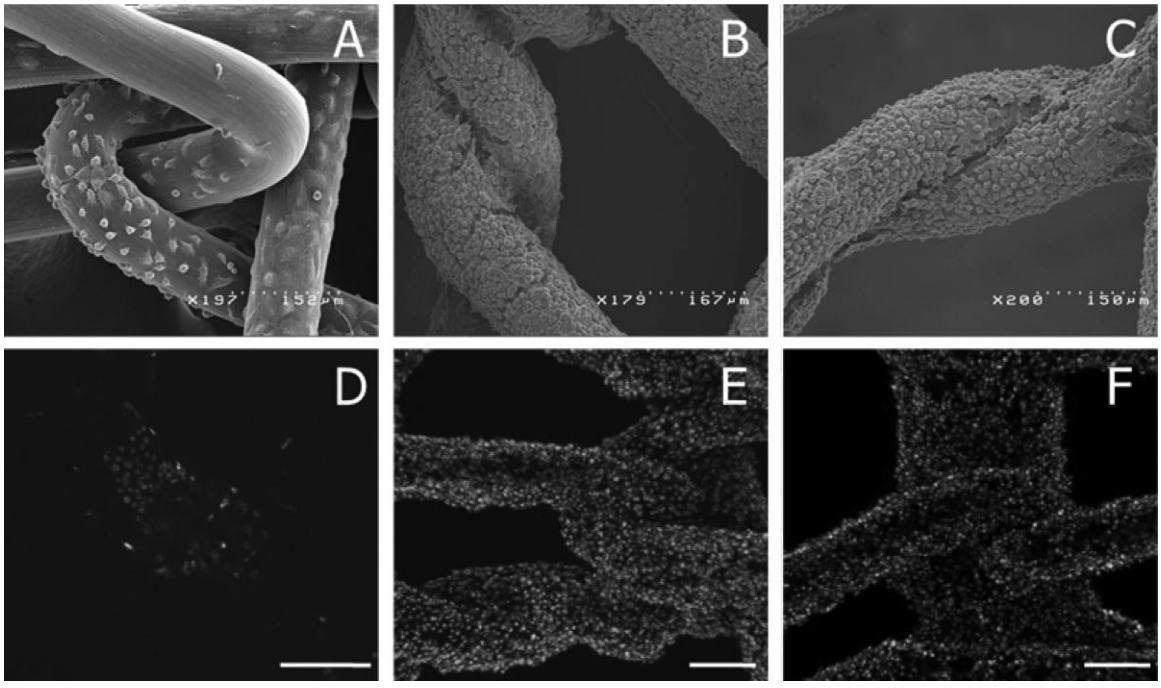

Figure 5. SEM pictures of PP meshes compared to PMA/PMMA- and DTPA-Gd- PMA/PMMA-coated meshes on day 8 (A, B and C, respectively). Confocal microscopy images of PP (D), PMA/PMMA (E), and DTPA-Gd-PMA/PMMA-coated (F) meshes after 8 d of incubation with L-929 cells and after live/dead staining. Scale bares represent 100 mm.

3.4. In vitro Colonization of MR-Visible Meshes

L-929 cells on coated meshes were examined for their morphology and viability (MTT test, live/dead staining and SEM) to evaluate to what extent MR-visible meshes are suitable for colonization, and the results were compared with those of native meshes.

The MTT tests indicated that L-929 cells adhered preferentiallyto thecoated meshes(DTPA-Gd-PMA/PMMA; abs. ¼ 0.35 and PMA/PMMA; abs. ¼ 0.36), compared to the native PP meshes (abs. ¼ 0.18). Hydrophobicity and cristallinity are physico-chemical factors known to impede cell interactions with materials.[35,36]

SEM investigations showthat L-929 cells proliferate slowly and with difficulty on the PP mesh surface. Bycontrast, PMA/PMMA- and DTPA-Gd-PMA/PMMA-coated meshes were entirely covered by L-929 cells after 8 d, and the cells showed typical morphology (Figure 5B and C). Observations by confocal microscopy on Live and Dead stained meshes illustrated the same phenomenon. A few cells were present on the PP mesh surface (Figure 5A and D) whereas the PMA/PMMA (Figure 5B and E) and DTPA-Gd-PMA/PMMA mesh surfaces (Figure 5C and F) were entirely colonized. Although no green/red ratio was determined to quantify cell vitality, red stained cells were seen to be slightly more dispersed on the material surface in the case of the MR-visible mesh (Figure 5F) compared to the Gd-free mesh (Figure 5E). However, this cell mortality may be due to the high cell density and the confluence observed on these meshes.

Even though PP materials are classified as inert and non-immunogenic, theirmaindrawbacks assurgicalmeshesare that they induce an inflammatory reaction – known as the foreign body reaction – which seems to be dependent on mesh weight,[37–40] and fibroblasts find it difficult to grow on the surface of PP meshes.[41] These drawbacks may hamper or delay mesh integration into tissue since it has been recognized that fibroblast proliferation is part of the first phase in the wound healing process.[42] Klinge et al. showed that implanted meshes induced acute and long-term inflammatory reactions that were dependent upon

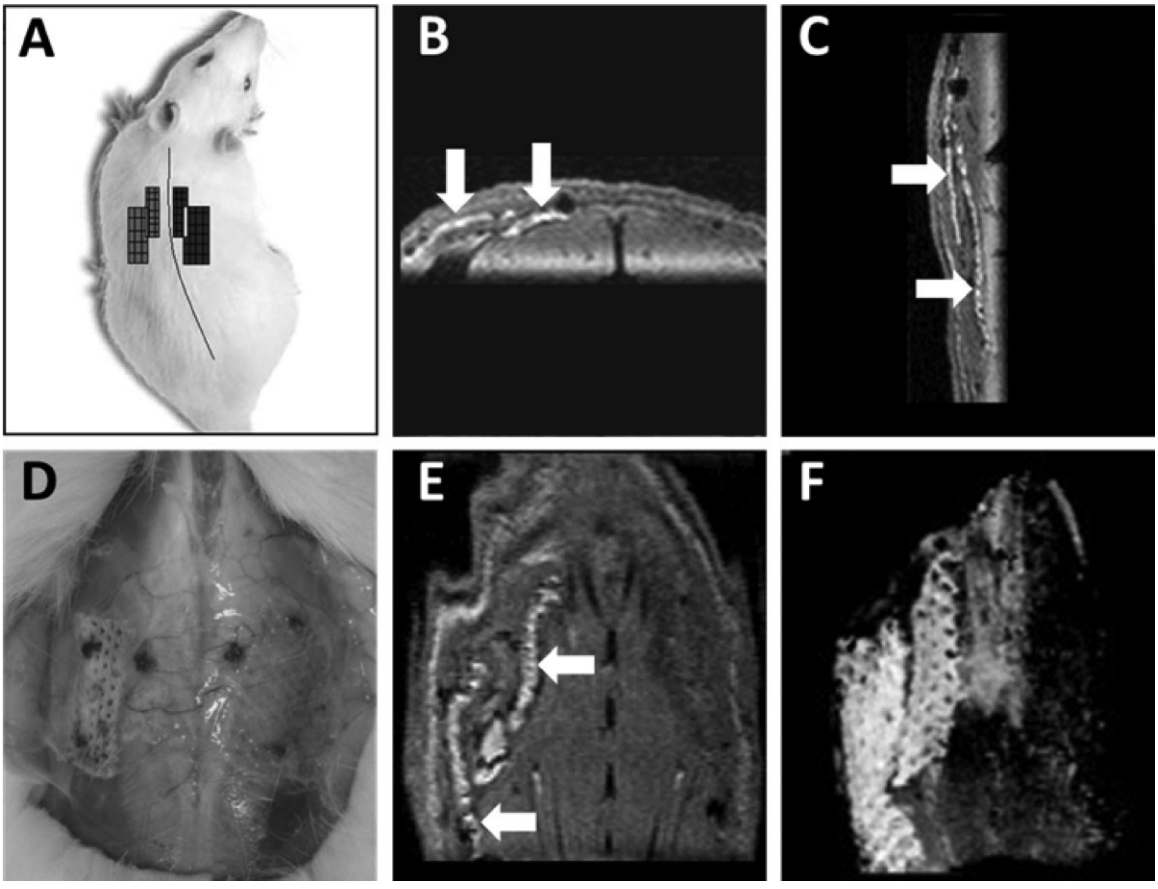

Figure 6. In vivo MRI visualization of meshes after implantation in rats. (A) Schematic presentation of mesh implantation sites. DTPA-Gd-PMA/PMMA-coated meshes were implanted on the left side and PMA/PMMA-coated meshes on the right, used as negative controls. (D) Anatomical location of the implanted meshes. Frames B, C, and E correspond to three orthogonal views (axial, sagittal, and coronal views, respectively) of the rat extracted from the 3D MRI dataset. Frame F corresponds to the MIP reconstruction processed from the 3D dataset.

mesh structure, and the amount and surface of mesh in contact with the host.[37,43,44] In view of the results of our in vitro colonization study, MR-visible coated meshes, compared to native PP meshes, are more liable to interact with cells and be colonized in vitro.

3.5. In vivo Visualization of DTPA-Gd-PMA-Coated Meshes

Two MR-visible meshes were implanted subcutaneously in rats on the left lumbar muscle whereas negative controls coated with PMA/PMMA were implanted similarly on the right (Figure 6A and D). The DTPA-Gd-PMA/PMMA-coated meshes were unambiguously visible by MRI one month after implantation while the negative controls, composed of PMA/PMMA, were not (Figure 6).

The DTPA-Gd-PMA/PMMA-coated meshes appeared as hyperintense linesasshowninthe axial, sagittal, and coronal views (Figure 6B, C, and E, respectively). The 3D MR dataset acquired was used to generate the MIP image and thus yield additional information about mesh morphology and their anatomical location (Figure 6F). Mesh curvature and shape together with exact location or proximity to organs and tissues such as blood vessels or spinal cord were easily visible (Video 2, available in the Supporting Information). This visualization, which is currently unavailable in medical imaging, would be of great benefit for surgeons and radiologists and would help understand and prevent the postoperative complications which frequently require mesh removal.

4. Conclusion

We have reported the synthesis and chemical characterization of a new MR-visible polymer based on PMA. This new polymer has been coated onto PP meshes, rendering them visible on a 7 T MRI Scanner. The synthesis, which uses covalent, non-hydrolyzable grafting of a chelate onto a PMA skeleton, prevents the release of gadolinium for at least 6 months, and this regardless of which sterilization procedure is employed. Cytocompatibility studies of the grafted polymer on L-929 fibroblasts showed that the DTPA-Gd-PMA coating does not significantly hamper cell adhesion, proliferation or vitality. To the best of our knowledge, this is the first time that a polymer prosthesis has been rendered MRI-visible in vivo thanks to a T1 signal enhancement. Our easy localization of the coated meshes after animal implantation clearly underlines the clinical benefits of this biomaterial which could be used to localize implanted devices, but also as MR-labeling for surgical sponges or other textiles retained in the body after surgery.

Acknowledgements: The authors are grateful to Dr. Chantal Cazevieille (CRIC, University Montpellier I), Dr. Nicole Lautredou and Dr. Julien Cau (Rio Imaging, Montpellier) for their technical assistance and interpretation of ultrastructural data, to Sylvie Hunger for 1H NMR analyses and to Dr. Olivier Bruguier (Geosciences, University Montpellier II) for his help in ICP-MS measurements. This work was partially supported by ''Agence Nationale de la Recherche'' grant no. ANR-08-TECS-020-01 and by the French Ministry of Education and Research for Sebastien Blanquer's fellowship. English has been reviewed by Mark Jones from Transcriptum (Avignon B 383 132 495–S.I.R.E.T. 383 132 495 00037).

Received: June 11, 2012; Published online: August 9, 2012; DOI: 10.1002/mabi.201200208

Keywords: DTPA; gadolinium; magnetic resonance imaging (MRI); polymer modification; prostheses

[1] B. Gallez, H. M. Swartz, *NMR Biomed.* 2004, *17*, 223.
[2] R. B. Lauffer, *Magn. Reson. Quarterly* 1990, *6*, 65.
[3] M. Boukerrou, P. Mesdagh, H. Yahi, G. Crepin, Y. Robert, M. Cosson, *Gynecol. Obstet. Fertil.* 2006, *34*, 1024.
[4] T. Fischer, R. Ladurner, A. Gangkofer, T. Mussack, M. Reiser, A. Lienemann, *Eur. Radiol.* 2007, *17*, 3123.
[5] J. F. Lapray, P. Costa, V. Delmas, F. Haab, *Prog. Urol.* 2009, *19*, 953.
[6] A. J. Maubon, M. P. Boncoeur-Martel, V. Juhan, C. R. Courtieu, A. S. Thurmond, P. Aubas, P. Mares, J. P. Rouanet, *Eur. Radiol.* 2000, *10*, 879.
[7] C. Birch, *Best Pract. Res. Clin. Obstet. Gynaecol.* 2005, *19*, 979.
[8] J. L. Bouillot, S. Servajean, N. Berger, N. Veyrie, D. Hugol, *Ann. Chir.* 2004, *129*, 132.
[9] D. Earle, J. Romanelli, *Contemp. Surg.* 2007, *63*, 63.
[10] S. Kos, R. Huegli, E. Hofmann, H. H. Quick, H. Kuehl, S. Aker, G. M. Kaiser, P. J. Borm, A. L. Jacob, D. Bilecen, *Cardiovasc. Intervent. Radiol.* 2008, *32*, 514.
[11] G.-P. Yan, L. Robinson, P. Hogg, *Radiography* 2007, *13*, e5.
[12] N. A. Kraemer, C. W. Hank, J. Otto, M. Hodenius, *Invest. Radiol.* 2010, *45*, 477.
[13] J. Otto, N. Krämer, A. Krombach, I. Slabu, M. Hodenius, M. Baumann, U. Klinge, in *Hernia Repair Sequelae*, (Eds., V. Schumpelick, D. P. FitzPatrick), Springer, Heidelberg 2010.
[14] J. O. DeLancey, *Clin. Obstet. Gynecol.* 1993, *36*, 897.
[15] V. V. Mody, M. I. Nounou, M. Bikram, *Adv. Drug Deliv. Rev.* 2009, *61*, 795.
[16] H. H. Chen, C. Le Visage, B. Qiu, X. Du, R. Ouwerkerk, K. W. Leong, X. Yang, *Magn. Reson. Med.* 2005, *53*, 614.
[17] A. L. Doiron, K. Chu, A. Ali, L. Brannon-Peppas, *Proc. Natl. Acad. Sci. U. S. A.* 2008, *105*, 17232.
[18] A. L. Doiron, K. A. Homan, S. Emelianov, L. Brannon-Peppas, *Pharm. Res.* 2008, *26*, 674.
[19] O. Unal, J. Li, W. Cheng, H. Yu, C. M. Strother, *J. Magn. Reson. Imaging* 2006, *23*, 763.
[20] J. Guo, X. Jiang, Y. Hu, C. Yang, *J. Mater. Sci. Mater. Med.* 2003, *14*, 283.
[21] J. Guo, J. Xiqun, *J. Appl. Polym. Sci.* 2002, *87*, 1358.
[22] X. Jiang, H. Yu, R. Frayne, O. Unal, C. M. Strother, *Adv. Mater.* 2001, *13*, 490.

[23] G. Ratzinger, P. Agrawal, W. Korner, J. Lonkai, H. M. Sanders, E. Terreno, M. Wirth, G. J. Strijkers, K. Nicolay, F. Gabor, *Biomaterials* 2010, *31*, 8716.
[24] L. Lemaire, A. Vonarbourg, A. Sapin, F. Franconi, P. Menei, P. Jallet, J. J. Le Jeune, *Magn. Reson. Mater. Phys. Biol. Med.* 2004, *17*, 133.
[25] X. Garric, H. Garreau, M. Vert, J. P. Moles, *J. Mater. Sci. Mater. Med.* 2007, *19*, 1645.
[26] T. Mosmann, *J. Immunol. Methods* 1983, *65*, 55.
[27] S. Ponsart, J. Coudane, M. Vert, *Biomacromolecules* 2000, *1*, 275.
[28] J. Coudane, B. Nottelet, A. El Ghzaoui, M. Vert, *Biomacromolecules* 2007, *8*, 2594.
[29] J. Coudane, B. Nottelet, M. Vert, *Biomaterials* 2006, *27*, 4948.
[30] S. Blanquer, O. Guillaume, V. Letouzey, L. Lemaire, F. Franconi, C. Paniagua, J. Coudane, X. Garric, *Acta Biomater.* 2012, *8*, 1339.
[31] T. Frenzel, P. Lengsfeld, H. Schirmer, J. Hutter, H. J. Weinmann, *Invest. Radiol.* 2008, *43*, 817.
[32] T. Grobner, *Nephrol. Dial. Transplant.* 2006, *21*, 1745.
[33] J. M. Idee, M. Port, I. Raynal, M. Schaefer, S. Le Greneur, C. Corot, *Fundam. Clin. Pharmacol.* 2006, *20*, 563.
[34] European Standard: Biological evaluation of medical devices Part 1: Evaluation and testing 2004 EN ISO 109931:2004
[35] D. Weyhe, I. Schmitz, O. Belyaev, R. Grabs, K. M. Muller, W. Uhl, V. Zumtobel, *World J. Surg.* 2006, *30*, 1586.
[36] V. Hendrick, E. Muniz, G. Geuskens, J. Werenne, *Cytotechnology* 2001, *36*, 49.
[37] U. Klinge, B. Klosterhalfen, V. Birkenhauer, K. Junge, J. Conze, V. Schumpelick, *J. Surg. Res.* 2002, *103*, 208.
[38] B. Klosterhalfen, B. Hermanns, R. Rosch, K. Junge, *Eur. Surg.* 2003, *35*, 16.
[39] A. Schachtrupp, U. Klinge, K. Junge, R. Rosch, R. S. Bhardwaj, V. Schumpelick, *Br. J. Surg.* 2003, *90*, 114.
[40] H. Scheidbach, C. Tamme, A. Tannapfel, H. Lippert, F. Kockerling, *Surg. Endosc.* 2004, *18*, 211.
[41] M. Kapischke, K. Prinz, J. Tepel, J. Tensfeldt, T. Schulz, *Surg. Endosc.* 2005, *19*, 791.
[42] W. K. Stadelmann, A. G. Digenis, G. R. Tobin, *Am. J. Surg.* 1998, *176*, 26s.
[43] U. Klinge, B. Klosterhalfen, M. Muller, M. Anurov, A. Ottinger, V. Schumpelick, *Biomaterials* 1999, *20*, 613.
[44] U. Klinge, B. Klosterhalfen, M. Muller, V. Schumpelick, *Eur. J. Surg.* 1999, *165*, 665.